Dynamics on the HOCO potential energy surface studied by dissociative photodetachment of $HOCO^-$ and $DOCO^-$

Zhou Lu, Qichi Hu, Jonathan E. Oakman, and Robert E. Continetti[a)]
Department of Chemistry and Biochemistry, University of California, San Diego, La Jolla, California 92093-0340

(Received 5 January 2007; accepted 26 March 2007; published online 16 May 2007)

An experimental study of the dissociative photodetachment (DPD) dynamics of $HOCO^-$ and $DOCO^-$ at a photon energy of 3.21 eV has been carried out to probe the potential energy surface of the HOCO free radical and the dynamics of the $OH+CO \rightarrow H+CO_2$ reaction. These photoelectron-photofragment coincidence experiments allow the identification of photodetachment processes leading to the production of stable HOCO free radicals and both the $H+CO_2$ and OH +CO dissociation channels on the neutral surface. Isotopic substitution by deuterium in the parent ion is observed to reduce the product branching ratio for the $D+CO_2$ channel, consistent with tunneling playing a role in this dissociation pathway. Other isotope effects on the detailed partitioning of kinetic energy between photoelectrons and photofragments are also discussed. The results are compared to recent theoretical predictions of this DPD process, and evidence for the involvement of vibrationally excited $HOCO^-$ anions is discussed. © *2007 American Institute of Physics*. [DOI: 10.1063/1.2731787]

I. INTRODUCTION

The hydroxyl formyl (HOCO) free radical is an important intermediate in the bimolecular reaction between the hydroxyl radical and carbon monoxide, $OH+CO \rightarrow H+CO_2$. Over the last three decades, this reaction has been the focus of intense interest as a result of its importance in determining the CO/CO_2 balance in combustion and atmospheric chemistry[1] and the role it plays in the release of heat during hydrocarbon combustion.[2] Extensive experimental and theoretical studies have sought to characterize the reaction kinetics and dynamics as well as the structure of the HOCO radical, making this system a benchmark four-atom reaction. In the present work, the dynamics on the HOCO potential energy surface was studied by preparing the HOCO free radical, its deuterated form DOCO, and the atomic and molecular dissociation products $H/D+CO_2$ and OH/OD+CO by the dissociative photodetachment (DPD) of $HOCO^-$ and $DOCO^-$.

Previous theoretical efforts on this system concentrated on the construction of an accurate potential energy surface (PES) for the ground electronic state ($X\,^2A'$) of the HOCO complex that governs the $OH+CO \rightarrow H+CO_2$ reaction. McLean and Ellinger reported *ab initio* predictions for the two planar isomers, *trans*- and *cis*-HOCO.[3,4] Several groups have studied the HOCO PES at different levels of *ab initio* and density functional theory (DFT) calculations. Some of these studies have focused particularly on the stationary points along the OH+CO reaction path.[5,6] The first global PES for the $H+CO_2$ reaction was presented by Schatz *et al.* in 1987, using singly and doubly excited configuration interaction calculations and a many-body expansion fit.[7] This surface has been improved several times over the following years.[8–11] A number of other attempts to develop partial or full-dimensional HOCO PESs have been made using a variety of different methods.[12–14] Most recently, a new high-level *ab initio* complete active space self-consistent field/multireference configuration interaction calculation with all 17 valence electrons and 13 valence orbitals included in the active space was performed by Song *et al.*, reporting a calculated heat of reaction of −24.1 kcal/mol at 0 K for $OH+CO \rightarrow H+CO_2$.[15] They also used these high-level reference calculations to assess new DFT approaches to calculate this PES.

The energetics of the HOCO system obtained from several recent high-level quantum calculations are summarized in Table I and Fig. 1, with the zero point energy (ZPE) corrected OH+CO products chosen as the reference. Although these theoretical predictions depend greatly on different calculation levels, it is well accepted that the *trans*-HOCO conformer is slightly lower in energy than *cis*-HOCO, with an isomerization barrier (TS in Fig. 1) estimated to be ~0.35 eV higher than *trans*-HOCO.[10,11,14,15] In the reaction of OH+CO, *trans*-HOCO is initially formed via a transition state (*t*-HOCO TS1), which is nearly isoenergetic with the OH+CO asymptote (see Table I),[10,14,15] then converts into the *cis*-HOCO conformer. The saddle point (*c*-HOCO TS2) separating the *cis*-HOCO complex and the reaction exit channel $H+CO_2$ is characterized by a high imaginary frequency ($2053i$ cm^{-1}) (Ref. 10) that is consistent with several predictions claiming that $H+CO_2$ products are formed by tunneling through the TS2 barrier.[6,12,16] In addition, two hydrogen bonded complexes OH···CO (hb1) and OH···OC (hb2) exist along the entrance channel OH+CO before the formation of *t*-HOCO TS1, which may play important roles in the abnormal temperature and pressure dependences of the reaction rate coefficients.[17,18] A less favorable reaction path

[a)]Electronic mail: rcontinetti@ucsd.edu

TABLE I. Theoretical prediction of relative energies for HOCO system (eV) [all energies have been corrected by ZPEs, OH+CO is used as reference, *t* stands for *trans* and *c* stands for *cis*].

	CCF[a]	DFF[b]	FDF[c]	LTSH[d]	YMS[e]	VHK[f]	SLHW[g]
OH+CO	0.00	0.00	0.00	0.00	0.00 (−0.06)	0.00	0.00
t-HOCO (TS1)					0.03 (−0.05)	0.04	−0.03
c-HOCO (TS1)					0.18 (0.11)	0.17	0.14
OHCO (hb1)					−0.04 (−0.12)	−0.01	−0.04
OHOC (hb2)					−0.01 (−0.08)	0.01	−0.01
t-HOCO (min)	−1.19	−1.10	−1.12	−1.31	−1.10 (−1.19)	−1.06	−1.00
c-*t*-HOCO (TS)			−0.87	−0.96	−0.75 (−0.83)	−0.73	−0.64
c-HOCO (min)	−1.11		−0.99	−1.21	−1.03 (−1.12)	−0.92	−0.92
c-H···OCO (TS2)				0.07	0.05 (0.03)	0.05	0.11
t-HOCO (TS4)				0.34	0.37 (0.33)	0.40	0.49
C_{2v}-HCO_2 (min)			−0.49	−0.63	−0.43 (−0.51)	−0.46	−0.47
C_{2v}-HCO_2 (TS)				−0.42	−0.45 (−0.47)	−0.44	−0.47
H···OCO (vdw)					−1.07 (−1.07)	−1.07	
$H+CO_2$					−1.07 (−1.07)	−1.07	−1.05
t-$HOCO^-$	−2.49	−2.46					
c-$HOCO^-$	−2.54	−2.52					
AEA *t*-HOCO	1.30	1.36					
AEA *c*-HOCO	1.43						

[a]CCF: Clements, Continetti, and Francisco, Ref. 60, the reference for the OH+CO asymptote was determined by the calculated energetics of OH^-+CO in Ref. 60 and the EA(OH)=1.8277 eV (Ref. 81).
[b]DFF: Dixon, Feller, and Francisco, Ref. 62.
[c]FDF: Feller, Dixon, and Francisco (Ref. 63). Note that $\Delta_f H^0$ (OH)=8.85±0.07 kcal/mol (Ref. 82) and a calculated $\Delta_f H^0$ (CO)=−27.0 kcal/mol (Ref. 63) was used to obtain the reference OH+CO asymptote in both DFF and FDF.
[d]LTSH: Lakin, Troya, Schatz, and Harding, Ref. 11.
[e]YMS: Yu, Muckerman, and Sears, Ref. 10, in parentheses, energetics of species involved in the OD+CO → D+CO_2 reaction.
[f]VHK: Valero, van Hemert, and Kroes, Ref. 14.
[g]SLHW: Song, Li, Hou, and Wang, Ref. 15.

involves *trans*-HOCO converting to the C_{2v} symmetry H·CO_2 conformer over a high barrier (TS4) with subsequent dissociation into $H+CO_2$.[8–10,15]

To evaluate these surfaces, one has to compare the theoretical predictions with experimental results. The HOCO complex and its deuterated form DOCO have been observed

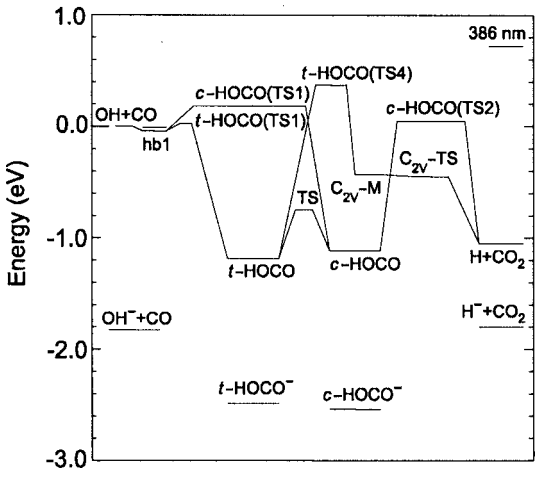

FIG. 1. Energy diagram for the OH+CO↔$HOCO^*$→$H+CO_2$ reaction and DPD of $HOCO^-$. All energies are in eV and corrected by ZPEs, the ground states of OH+CO are selected as reference. Energetics of OH^-+CO, as well as anionic and neutral HOCO minima, are from Ref. 60; the EA of H atom, 0.754 eV (Ref. 83) was used to determine the stability of H^-+CO_2; the energies of other species here are from Ref. 10. The photon energy here is in reference to *trans*-$HOCO^-$.

in cryogenic matrices[19–21] and the gas phase,[22–29] and their rotational[23–28] and vibrational frequencies[19–21] have been reported and can be directly compared with calculated values. Lester and co-workers reported spectroscopic evidence for the OH···CO complex in the OH+CO entrance channel.[18,30,31] Additionally, significant experimental and theoretical efforts have been carried out to study the pressure and temperature dependences of the rate coefficient of the OH+CO reaction, providing evidence for a deep HOCO well and a high barrier leading to the formation of $H+CO_2$.[6,16,32–39] The OH+CO (Refs. 40–43) and $H+CO_2$ (Refs. 44–48) collisions have been studied by various experimental techniques as well, yielding cross sections and internal energy distributions in reaction products. These experimental results can be compared with theoretical predictions based on *ab initio* PESs and classical/quasiclassical trajectory theories[8,9,11,17,49,50] or quantum dynamics calculations.[49–56]

However, there remains a lack of detailed and direct measurement of the global HOCO PES. For instance, it is difficult to measure the depth of the HOCO potential well accurately. Early attempts were made to obtain a heat of formation of the HOCO radical by measuring the appearance potential of $C_2H_5^+$ from electron impact of $C_2H_5CO_2H$ or CH_3^+ from CH_3CO_2H,[57,58] reporting $\Delta_f H^0$ to be −39 and −58±4 kcal/mol, respectively. Ruscic *et al.* obtained $\Delta_f H^0$ =−52.5±0.6 kcal/mol directly by the photoionization of the HOCO radical.[22] Later this value was revised to be $\Delta_f H^0$

$\geqslant -45.8 \pm 0.7$ kcal/mol using the same technique,[59] yielding a HOCO well depth less than 1.20 eV relative to the OH+CO asymptote. In addition, the role of a tunneling mechanism for the production of $H+CO_2$ has been debated in different studies,[6,16,32–36,41] and a direct measurement of the height of the various transition states on this PES has yet to be completed.

Recently the dynamics and PES of the HOCO free radical were studied by Clements *et al.* using DPD of the anion precursor $HOCO^-$.[60] Using photoelectron-photofragment coincidence (PPC) spectroscopy, three product channels after the photodetachment of $HOCO^-$ with 4.80 eV (258 nm) photons were reported:

$$HOCO^- + h\nu \rightarrow HOCO + e^-, \quad (1)$$

$$HOCO^- + h\nu \rightarrow OH + CO + e^-, \quad (2)$$

$$HOCO^- + h\nu \rightarrow H + CO_2 + e^-. \quad (3)$$

While the majority of photodetachment products are stable HOCO radicals, unimolecular dissociation into $H+CO_2$ and OH+CO fragments, as well as the evidence for direct DPD on a repulsive excited electronic state yielding ground state $OH+CO+e^-$, were observed.

The DPD studies are based on the discovery and characterization of a stable, bound $HOCO^-$ anion precursor. The first experimental evidence for this species was reported in flowing afterglow experiments studying the hydroxide-transfer reaction of H_3O^-+CO and indicated the presence of a negative ion with $m/e=45$ that was determined not to be the more stable formate anion, HCO_2^-.[61] Interpretation of the DPD experiments was aided by high-level *ab initio* calculations on $HOCO^-$ and HOCO by Clements *et al.*[60] The adiabatic electron affinities (AEAs) of the two HOCO isomers were predicted to be 1.43 eV (*cis*) and 1.30 eV (*trans*), respectively from CCSD(T) calculations [Clements, Continetti, and Francisco (CCF), see Table I], which agrees well with the DPD measurements.[60] The same calculation predicted a deeper neutral HOCO well compared with most of the other calculations listed in Table I, except for the Lakin, Troya, Schatz, and Harding (LTSH) results. Dixon *et al.* recently predicted an AEA for *trans*-HOCO of 1.36 eV as well as the energy of the *cis* anion [see Dixon, Feller, and Francisco (DFF) results in Table I].[62] These authors reported the energetics of both *cis*- and *trans*-HOCO radicals using a slightly different theoretical approach elsewhere [see Feller, Dixon, and Francisco (FDF) results in Table I],[63] with a 0.02 eV difference seen between the depth of the *trans*-HOCO well reported in the DFF (Ref. 62) and FDF results.[63] Therefore, an accurate prediction for the AEA of the *cis* conformer is not available in the recent work of Dixon and co-workers. In addition, the anion stability relative to the OH+CO asymptote predicted by CCF and DFF only differs by 0.03 and 0.02 eV for the *trans*- and *cis*-$HOCO^-$ isomers, respectively (see Table I). Thus, we will continue to use the consistent level of theory for both anions and neutrals reported by CCF.

The previous DPD study provided important experimental information on the HOCO PES. However, there are several questions remaining unanswered, in particular, the role played by tunneling in the dissociation to $H+CO_2$, the observation of a significant fraction of the $OH+CO+e^-$ products at total kinetic energies beyond the calculated energetic maximum, and a detailed comparison of the product branching ratios with statistical and quantum dynamical predictions. To achieve a better understanding of the reaction mechanisms and energetics of this system, in the current work we compare the DPD dynamics of the deuterated anion $DOCO^-$ with $HOCO^-$ at a photodetachment wavelength of 386 nm ($E_{h\nu}=3.21$ eV). The use of a longer wavelength in this study removes potential contributions from excited electronic states of HOCO and provides improved photoelectron kinetic energy resolution. Following a brief review of the experimental technique, the photoelectron spectra corresponding to channel (1) and the PPC spectra arising from the DPD channels (2) and (3) for both isotopologs will be presented, as well as the branching ratios for the three neutral product channels. The observed isotope effects and inferred DPD mechanisms will be discussed in detail and compared with recent theoretical predictions by Zhang *et al.*[64]

II. EXPERIMENT

The fast-ion-beam PPC spectrometer employed in the present study is capable of measuring angle-resolved photoelectron and photofragment kinetic energies from a single DPD event in coincidence, allowing a direct probe of the dissociation dynamics on the neutral PES after photodetachment.[65] The experimental approach is similar to the previous DPD study by Clements *et al.*[60] with the exception that a new multiparticle photofragment imaging detector was used in this study and the photoelectron spectra were solely recorded by an imaging detector. Therefore only a brief review of experimental method will be presented here. In the final measurements reported here, the $HOCO^-$ anion ($m/e=45$) was created using electron impact on a 1 kHz pulsed supersonic expansion of 7% CO, 6% N_2O, 17% CH_4, and 70% N_2. For the $DOCO^-$ experiments, CD_4 (99%, Cambridge Isotope Laboratory) instead of CH_4 was used in the precursor gas mixture. Here N_2 was used to dilute the gas mixture and assist the collisional cooling in supersonic expansion. An alternative experiment without N_2 showed no observable difference, ruling out the involvement of $OH^-(N_2)$ species ($m/e=45$) in the present study. A plausible mechanism for the generation of the $HOCO^-$ anion involves electron impact on the N_2O/CH_4 mixture forming OH^- followed by the association of OH^- with CO to form $HOCO^-$ in the free-jet expansion. The nozzle-skimmer distance used in these experiments was 1.5–2.0 cm, and an interesting observation was made that $HOCO^-$ was formed most effectively when the electron beam was closer to the skimmer aperture. Thus, the condensation of neutrals into clusters followed by electron impact on those clusters may play an important role in the production of $HOCO^-$. After passing into a differentially pumped chamber, the anions were accelerated to 10 keV and mass selected by time of flight before being intercepted by a linearly polarized laser. The second harmonic (386 nm, $E_{h\nu}=3.21$ eV) of a pulsed Ti:sapphire laser

(Clark-MXR CPA-2000, 1.8 ps full width at half maximum, $\sim 1 \times 10^{10}$ W/cm^2) was used for photodetachment.

The full 4π *sr* solid angle of photoelectrons was collected by a space focusing electron optics assembly.[66,67] The time- and position-sensitive photoelectron detector allows the measurement of three-dimensional (3D) photoelectron velocities and is positioned parallel to the plane of the ion and laser beams. The photoelectron kinetic energy (eKE) resolution can be improved by discarding events with significant photoelectron velocity components perpendicular to the plane of the electron detector. The resulting photoelectron intensity distribution in these equatorially sliced photoelectron spectra is corrected based on the cylindrical symmetry about the electric vector of the laser when the laser polarization is along the ion beam and parallel to the face of the electron detector.[68] The photoelectron kinetic energy (eKE) resolution is $\Delta E/E \sim 13\%$ determined by the photodetachment of OH^- at 386 nm (eKE=1.38 eV).

Undetached anions were deflected out of the fast beam, while the neutral products impinged on a time- and position-sensitive detector which consists of a stack of microchannel plates and a fast-delay-line anode.[69] Stable neutral products (HOCO radicals) arrive at the detector at a time and position determined by the velocity vector distribution that characterizes the parent $HOCO^-$ ion packet prior to photodetachment. In the case of DPD, the time of arrival of two coincident photofragments has to differ by more than an ~17 ns dead time of the detector. The mass ratio of the coincident photofragments ($H+CO_2$ or $OH+CO$) and the center of mass (c.m.) kinetic energy release were determined by the conservation of linear momentum using the time- and position-of-arrival information.[70,71] One has to be cautious about the large false coincidence rate in the DPD process of $HOCO^-$ as the majority neutral products are stable HOCO free radicals and the kinetic energy release among dissociation fragments is small. An additional gating on the photofragment mass spectra was applied in data analysis procedure, reducing the false coincidence contribution to the data significantly. As a result of the large difference in masses for the $H+CO_2$ product channel, a large fraction of the H atom products miss the detector even at a beam energy of 10 keV, so the detector acceptance function (DAF), as well as the low detection efficiency for H atoms with microchannel-plate detectors,[72] plays an important role in the detection of this product channel. A Monte Carlo simulation has been used to calculate the DAF of the present spectrometer under these experimental conditions and correct the intensity distributions in the two dissociation product channels.[73] The DPD of O_4^- at 532 nm was used to calibrate the neutral particle detector, yielding a resolution of $\Delta E_T/E_T \sim 9\%$.

III. RESULTS

In accord with the previous DPD study using 4.80 eV photons, three neutral product channels were observed after the photodetachment of $HOCO^-$ or $DOCO^-$ at 3.21 eV. In this section, the experimental results for $H/D+CO_2+e^-$, $OH/OD+CO+e^-$, and $HOCO/DOCO+e^-$ channels will be presented separately, including the PPC spectra for both DPD channels and photoelectron spectra for the stable HOCO/DOCO channel.

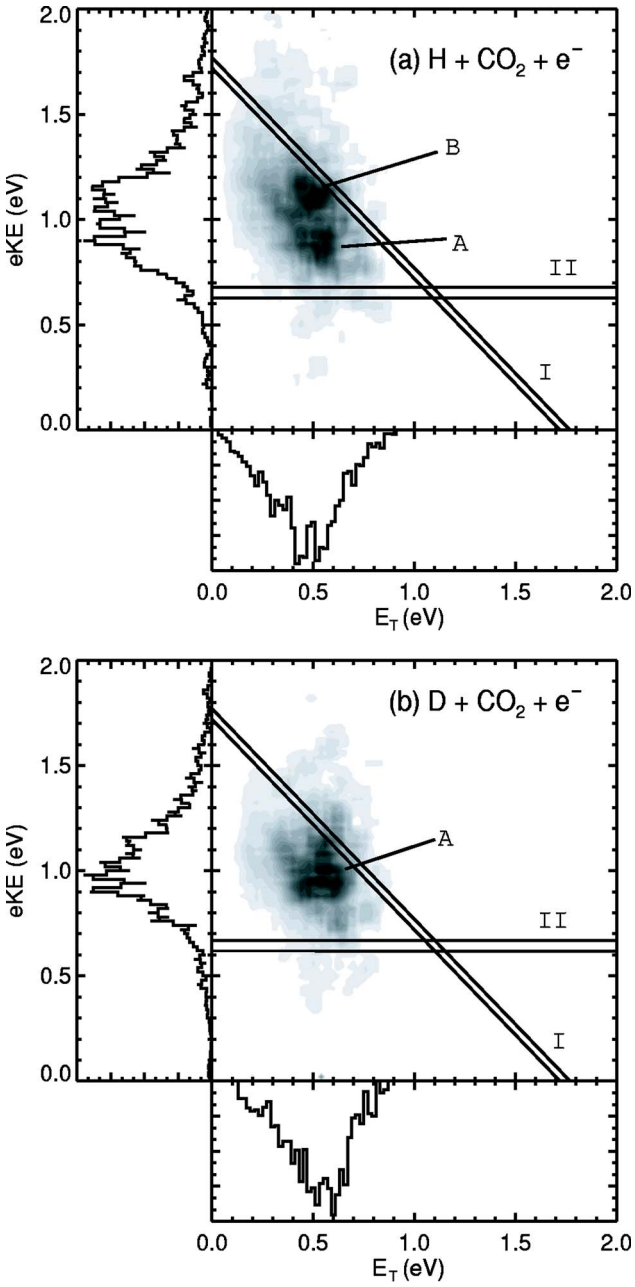

FIG. 2. Photoelectron-photofragment kinetic energy correlation spectra $P(\mathrm{eKE}, E_T)$ for (a) $HOCO^- + h\nu \rightarrow H + CO_2 + e^-$ and (b) $DOCO^- + h\nu \rightarrow D + CO_2 + e^-$ at $E_{h\nu}$=3.21 eV. In both (a) and (b) The diagonal lines 1 correspond to the theoretically predicted maximum kinetic energy release (KE_{max}) (Ref. 60) for the production of ground state $H+CO_2+e^-$ from ground state *trans*- and *cis*-$HOCO^-$. Horizontal lines II represent the predicted eKE for nascent HOCO radicals with the same energy as the *c*-HOCO TS2 barrier in Fig. 1, assuming the parent anions are vibrationally "cold," as discussed in the text.

A. $H/D+CO_2+e^-$ channel

The PPC spectra $P(\mathrm{eKE}, E_T)$ for the $H+CO_2+e^-$ and $D+CO_2+e^-$ channels resulting from the DPD of $HOCO^-$ and $DOCO^-$, respectively, are shown in Fig. 2. The PPC spectrum is a two-dimensional histogram where the intensity

of each point represents the probability for the observation of an event with a specific partitioning of kinetic energy between the photoelectron (eKE) and the recoil of the neutral photofragments (E_T) in the c.m. frame. The photoelectron spectrum P(eKE) displayed on the left side and the photofragment translational energy spectrum $P(E_T)$ on the bottom of the coincidence spectrum are generated by integrating over the complementary variable in the two-dimensional spectrum. As mentioned in the experimental section, only a small fraction of H products can be detected, making it necessary to DAF correct the raw coincidence spectra $N(\text{eKE},E_T)$ to generate the final $P(\text{eKE},E_T)$ in Fig. 2. The coincidence spectra presented here are truncated at $E_T=0.025$ eV. This is necessary because the DAF around $E_T=0$ rapidly approaches zero due to the dead time of the neutral particle detector and false coincidences from stable HOCO radicals increase when E_T is close to zero. As a result, the DAF corrected spectra are accompanied by an artificially high intensity at very small E_T. The equatorial slicing of photoelectron velocities is not used in the PPC spectra. Therefore the $P(\text{eKE},E_T)$ distributions presented here provide a complete kinematic description of the DPD process.

The two closely spaced diagonal lines I in Fig. 2 are theoretical predictions for KE_{max}, the maximum kinetic energy release for all products (eKE$+E_T$) in the DPD process $\text{HOCO}^-+h\nu\rightarrow\text{H}+\text{CO}_2+e^-$ at $E_{h\nu}=3.21$ eV. The two predicted KE_{max} values, 1.72 eV for *cis*-HOCO^- and 1.77 eV for *trans*-HOCO^-, are determined in the manner described by Clements *et al.*[60] In the present experiments, there is no clear way to determine the relative population of these predicted isomers in the parent ion beam. Since no theoretical calculations on DOCO^- are available, the KE_{max} values calculated for DPD of HOCO^- are also used in Fig. 2(b), showing the energetic limits qualitatively. More events extend beyond KE_{max} in $\text{D}+\text{CO}_2+e^-$ than in $\text{H}+\text{CO}_2+e^-$, because the deuterated experiment was carried out at a higher signal counting rate to minimize the consumption of the isotopic gas mixture, leading to a larger contribution of false coincidences.

Isotope effects in the DPD channel of $\text{HOCO}^-+h\nu\rightarrow\text{H}+\text{CO}_2+e^-$ can be examined by comparing Figs. 2(a) and 2(b). The photoelectron kinetic energy spectrum correlated with the $\text{H}+\text{CO}_2$ neutral product channel has a relatively broad distribution and a peak at ~1.1 eV, while the P(eKE) distribution in the $\text{D}+\text{CO}_2+e^-$ channel is obviously narrower, with a peak at ~1.0 eV. In the $P(E_T)$ spectrum for $\text{H}+\text{CO}_2$ neutral fragments, in addition to the two features at 0.43 and 0.52 eV, some evidence for a progression in the product CO_2 bending mode (~0.08 eV) (Ref. 74) is observed. This progression is similar to the previous observation in a study of the DPD of HCO_2^-, the formate anion isomer of HOCO^-.[75] It should be noted, however, that the formate anion has an EA ~ 3.49 eV (Ref. 76) and as a result has a very different photoelectron spectrum that cannot contribute to the present observations given a photon energy of 3.21 eV. Figure 2(b) shows that a similar $P(E_T)$ spectrum was observed for the $\text{D}+\text{CO}_2$ neutral products from DPD of DOCO^-, with the two major peaks shifted to 0.49 and 0.56 eV, respectively.

The horizontal line set II at eKE=0.67 eV (*trans*-HOCO^-) and 0.62 eV (*cis*-HOCO^-) in Fig. 2 shows the dissociation barrier *c*-HOCO TS2 into $\text{H}+\text{CO}_2$ products as predicted by *ab initio* calculations of TS2 (Ref. 10) and the ground state anions.[60] It is evident that nearly all of the eKE distribution is at higher energies than this limit, implying that dissociation into $\text{H}+\text{CO}_2$ occurs *below* the calculated TS2 barrier using the assumption that the parent HOCO^- anions have no internal excitation prior to photodetachment. This and other aspects of these spectra will be addressed further in Sec. IV.

B. OH/OD+CO+e^- channel

DPD of HOCO^- into $\text{OH}+\text{CO}+e^-$ was also observed. Figure 3 shows the PPC spectra $P(\text{eKE},E_T)$ for DPD of (a) $\text{HOCO}^-+h\nu\rightarrow\text{OH}+\text{CO}+e^-$ and (b) $\text{DOCO}^-+h\nu\rightarrow\text{OD}+\text{CO}+e^-$. The calculated energetic limitations KE_{max} (0.72 eV for *trans*-HOCO^- and 0.67 eV for *cis*-HOCO^-)[60] are marked by diagonal lines I. As Fig. 3 shows, most of the $\text{OH}+\text{CO}+e^-$ events have a total kinetic energy ($\text{KE}_{\text{total}}=\text{eKE}+E_T$) larger than the theoretical value of KE_{max}. The line set II in Fig. 3 shows the experimental KE_{max} values, ~1.25 eV for $\text{OH}+\text{CO}+e^-$ and ~1.30 eV for $\text{OD}+\text{CO}+e^-$, respectively, which are determined from the contour at 15% of peak and represent the estimated level of false coincidences. Such significant disagreement between the absolute theoretical energy limits and the experimental results was not observed in the $\text{H}+\text{CO}_2+e^-$ DPD channel, although this discrepancy is similar to the observation that the $\text{H}+\text{CO}_2+e^-$ channel appears to occur below the *c*-HOCO TS2 barrier on the PES. To compare the current work with the previous DPD study of HOCO^- at $E_{h\nu}=4.80$ eV, the maximum available energies (1.78 eV for *cis*- and 1.91 eV for *trans*-HOCO^-) predicted for photodetachment from the ground state of HOCO^- to the bottom of the neutral HOCO well (CCF calculation) (Ref. 60) are also shown in Fig. 3 by lines III.

The isotope effects on the $\text{OH}+\text{CO}+e^-$ channel are not as obvious as those observed in $\text{H}+\text{CO}_2+e^-$. A Gaussian fit to the overall profile in the P(eKE) spectra correlated with the OH+CO and OD+CO neutral products yields peaks of 0.73 and 0.76 eV, respectively. However, the most intense part of the PPC spectrum for $\text{OD}+\text{CO}+e^-$ [Fig. 3(b)] definitely is displaced farther from line set I toward higher eKE compared with the PPC spectrum for $\text{OH}+\text{CO}+e^-$ [Fig. 3(a)]. In the P(eKE) spectra for $\text{OH}+\text{CO}+e^-$, three barely resolved peaks are seen to be spaced by 0.08–0.09 eV from each other, in agreement with the predicted C–O′ stretching frequency in HOCO^- (663 cm^{-1} for *trans*- and 741 cm^{-1} for *cis*-HOCO^-) (Ref. 60) where O′ represents the O atom connecting the C and H atoms. Evidence for at least two of these three peaks is also observed with a shift to higher eKE in the P(eKE) distribution for $\text{OD}+\text{CO}+e^-$. The shapes of $P(E_T)$ for the OH+CO and OD+CO channels are very similar, with peaks at 0.12 and 0.15 eV, respectively.

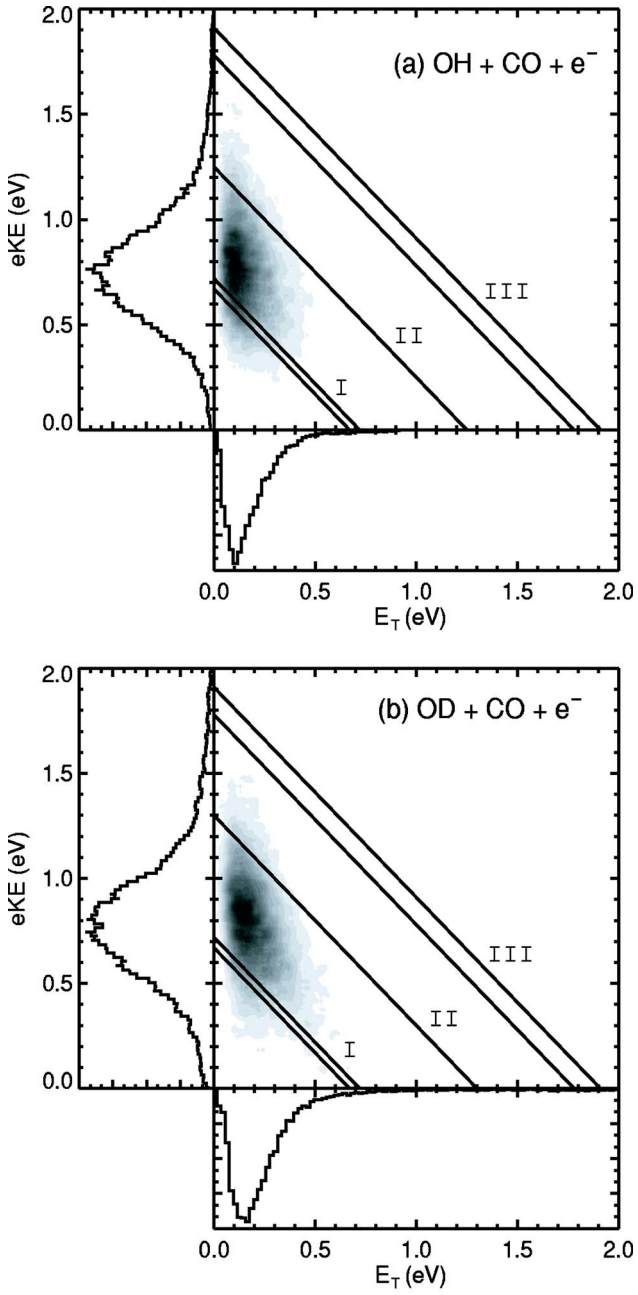

FIG. 3. Photoelectron-photofragment kinetic energy correlation spectra $P(\mathrm{eKE},E_T)$ for (a) $\mathrm{HOCO}^-+h\nu\rightarrow\mathrm{OH}+\mathrm{CO}+e^-$ and (b) $\mathrm{DOCO}^-+h\nu\rightarrow\mathrm{OD}+\mathrm{CO}+e^-$ at $E_{h\nu}$=3.21 eV. In both (a) and (b), the diagonal lines 1 correspond to the theoretical predictions of $\mathrm{KE}_{\mathrm{max}}$ for the production of ground state $\mathrm{OH}+\mathrm{CO}+e^-$ from the vibrationally "cold" *trans-* and *cis-*HOCO^- anions, respectively.[60] The diagonal line II corresponds to the experimental value of $\mathrm{KE}_{\mathrm{max}}$. The diagonal lines III represent the predicted maximum available energy for the photodetachment of ground state *trans-* and *cis-*HOCO^- to the bottom of the corresponding HOCO well.[60]

C. Stable HOCO+e^-

As discussed in the Introduction, the photodetachment of HOCO^- not only leads to the two DPD channels $\mathrm{OH}+\mathrm{CO}+e^-$ and $\mathrm{H}+\mathrm{CO}_2+e^-$ but predominantly yields the stable HOCO free radical. Figure 4(a) shows the overall photoelectron spectrum P(eKE) recorded in coincidence with either one or two neutral particles from the photodetachment of HOCO^-. This spectrum contains contributions from both stable and dissociative photodetachment, including dissociative events where only one of the atomic or molecular products is detected. The P(eKE) peaks in Fig. 4(a), at 1.18 eV for HOCO^- and 1.22 eV for DOCO^-, respectively, are at significantly higher eKEs compared to either of the DPD channels $\mathrm{H/D}+\mathrm{CO}_2+e^-$ and $\mathrm{OH/OD}+\mathrm{CO}+e^-$. As discussed by Clements *et al.*, this is consistent with the production of stable HOCO/DOCO radicals.[60]

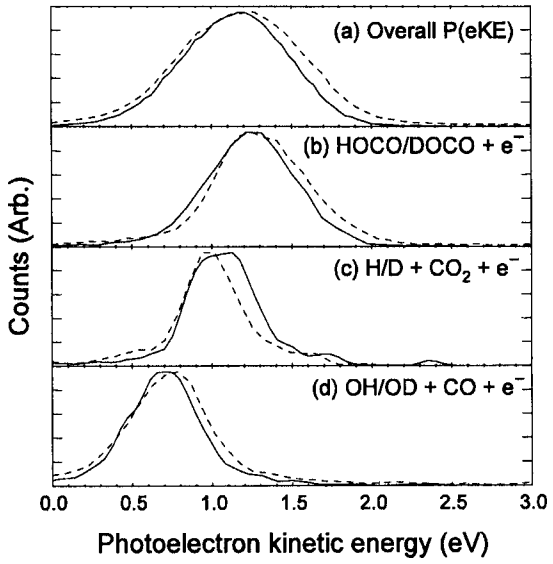

FIG. 4. Photoelectron kinetic energy spectra P(eKE) from the photodetachment of HOCO^- (solid lines) and DOCO^- (dashed lines): (a) overall P(eKE) observed in experiment; (b) P(eKE) spectra in coincidence with stable HOCO/DOCO; (c) P(eKE) in coincidence with $\mathrm{H/D}+\mathrm{CO}_2$; and (d) P(eKE) in coincidence with OH/OD+CO.

An analysis of the P(eKE) distributions coincident with only stable HOCO radicals was carried out by including only photoelectrons detected in coincidence with a single neutral particle. In addition, for any neutral particle taken into account as a stable HOCO radical, the reconstructed 3D position of arrival at the detector was required to fall within a small ($r\leqslant 1$ mm) spherical region centered on the parent ion beam. This effectively reduces false coincidence contributions to the stable HOCO spectrum from DPD events where only one particle, which in general recoils out of this spherical region, is detected. False coincidence contributions for the $\mathrm{H/D}+\mathrm{CO}_2$ channel will remain the largest, however, given the low detection efficiency for the H/D atoms and the fact that the recoil of CO_2 out of the ion beam is small. The resulting P(eKE) spectra shown in Fig. 4(b) are shifted to higher eKE, with the peaks at 1.29 eV for stable HOCO $+e^-$ and 1.32 eV for stable $\mathrm{DOCO}+e^-$. The eKE spectra from $\mathrm{H/D}+\mathrm{CO}_2+e^-$ and $\mathrm{OH/OD}+\mathrm{CO}+e^-$ are also summarized in Figs. 4(c) and 4(d), showing that distinct yet overlapping eKE spectra are observed for the three competing neutral product channels.

IV. DISCUSSION

The DPD of HOCO^- and its deuterated form allows a direct examination of theoretical predictions of the energetics and dynamics of the HOCO free radical and the potential energy surface governing the $\mathrm{OH}+\mathrm{CO}\rightarrow\mathrm{H}+\mathrm{CO}_2$ reaction. In this section, first the theoretical studies of this system will

be used to examine the mechanisms responsible for the observations presented here. Special attention will be paid to the potential role of vibrationally excited anions in both of the DPD channels and the tunneling mechanism in the $H/D+CO_2$ channel. The isotope effects observed in the $P(eKE,E_T)$ coincidence spectra for $HOCO^-/DOCO^-$ will be discussed as well. Finally, the branching ratios for the three neutral product channels after the photodetachment of $HOCO^-/DOCO^-$ will be compared with the theoretical predictions from the most recent six-dimensional quantum wave packet dynamics calculations.[64]

Only the ground electronic state of the HOCO radical can be accessed by the photodetachment of the $HOCO^-$ anion at $E_{h\nu}=3.21$ eV.[60] Although all of the energy minima and saddle points shown in Fig. 1 are energetically allowed, the region of the PES where nascent HOCO radicals can be produced is restricted by the Franck-Condon overlap determined by the structure of the parent anion. The HOCO radicals with the highest energy on the PES can be expected to lead to $OH+CO+e^-$ products, in competition with the more thermodynamically favorable dissociation channel leading to $H+CO_2+e^-$. Those nascent HOCO intermediates possessing the lowest energy (highest eKE) are trapped inside the deep potential well and form stable free radicals.

As mentioned in Sec. II, with the assumption that all the anions before photodetachment are in the vibrational ground state, nearly all of the $H+CO_2+e^-$ products will be formed below the *c*-HOCO TS2 barrier but have enough energy to surmount the $H\cdot CO_2$ barrier connecting the $C_{2v}H\cdot CO_2$ local minimum to $H+CO_2$ products. As noted before, the $P(E_T)$ distributions for $H+CO_2$ are found to be similar to those obtained from the DPD study of HCO_2^-,[75] making it necessary to examine the possibility that HOCO intermediates dissociate into $H+CO_2$ over the $H\cdot CO_2$ barrier, instead of passing through the most favorable reaction path involving *c*-HOCO TS2 expected for a parent $HOCO^-$ anion.

DPD of the HCO_2^- anion can be ruled out because the 3.21 eV photon energy used in these experiments is less than the 3.49 eV required to photodetach HCO_2^-.[76] Forming the $C_{2v}H\cdot CO_2$ conformer via *trans*-HOCO (the expected route) is not likely either, as this isomerization involves a high calculated barrier TS4, inconsistent with the observed photoelectron spectra which show that all the HOCO intermediates are produced with internal energies below TS4. Therefore the involvement of the $H\cdot CO_2$ barrier in $H+CO_2$ dissociation can be ruled out assuming the parent anions are vibrationally "cold."

If the anions were vibrationally excited, it would require 1.2 eV vibrational excitation in *trans*-$HOCO^-$ to overcome the TS4 barrier and yield the $P(eKE)$ spectrum seen in this experiment or 1.5 eV excitation in HCO_2^- to produce a $P(eKE)$ peak at 1.1 eV. The first case is impossible since *trans*-$HOCO^-$ would dissociate into OH^-+CO or H^-+CO_2 with such high excitation (see Fig. 1).[60] For the second case regarding HCO_2^-, even if the anions can be thermally excited by 1.5 eV, the low-lying excited electronic states of HCO_2 radical would be involved on the neutral PES generated by the photodetachment, and as a result a significantly different $P(eKE)$ spectrum from Fig. 4(c) would be expected.[75,76] Thus, the $H\cdot CO_2$ barrier is not likely to play a role in the production of $H+CO_2$ in this experiment.

A second explanation is that $H+CO_2$ products are formed by tunneling through the *c*-HOCO TS2 barrier. Several previous studies have suggested that the production of $H+CO_2$ by tunneling may play an important role in the OH+CO reaction.[6,12,16,37] However, the tunneling effect cannot explain why the other DPD channel $OH+CO+e^-$ is observed beyond the maximum energetic limits dictated by the available thermochemical data and theoretical predictions. Assuming that the theoretical calculations are correct, this disagreement can only be explained by the existence of either vibrationally excited $HOCO^-$ or other, unknown, anion isomers or excited electronic states with energies higher than the theoretically predicted *cis*- and *trans*-$HOCO^-$ isomers. Examination of the experimental KE_{max} in the $OH+CO+e^-$ channel [line II in Fig. 3(a)] shows that if this unknown anion isomer exists, its stability relative to $OH+CO+e^-$ will be roughly −2.0 eV, only ~0.2 eV below the OH^-+CO reactants. Therefore the potential involvement of weakly bonded $(OH^-)CO$ species in the $HOCO^-$ beam must also be considered. However, as noted in the earlier study by Clements *et al.*, the photoelectron angular distribution (PAD) for $HOCO^-$ peaks parallel to the laser electric vector. This is inconsistent with a weakly perturbed OH^- species as the PAD of OH^- is perpendicular to the laser polarization.[77] There is no theoretical evidence for the other anion isomer conformers such as $HOOC^-$ or $OHCO^-$ to date, although they cannot be completely ruled out.

Clements *et al.* proposed that either false coincidences with stable HOCO radicals or vibrationally excited $HOCO^-$ must be responsible for the significant discrepancy between the experimental and theoretical KE_{max} in the $OH+CO+e^-$ channel. The longer wavelength used for photodetachment in the present work allows a more accurate measurement of the photoelectron spectra and more effective discrimination against false coincidences with additional mass gating. The most likely mechanism for the observed spectra, therefore, is the presence of vibrationally excited $HOCO^-$ in the ion beam. The evidence of hot bands in parent ions has been observed in a previous experiment studying the photodetachment of $CH_3CO_2^-$ at 355 nm. An unresolved long tail in the near-threshold region of eKE spectrum[78] was later proved to be the mixing of vibrational progressions of OCO bending in CH_3CO_2 radical and hot bands of $CH_3CO_2^-$ by a photodetachment study of low-temperature $CH_3CO_2^-$.[79] The influence of hot bands may be more severe in the present study. As noted in the experimental section, when generating $HOCO^-$, a relatively long nozzle-skimmer distance was used, with electron impact localized near the skimmer aperture. Thus, collisional cooling of nascent $HOCO^-$ may not be effective in the limited expansion remaining. In another experiment studying the near-threshold photodetachment of $HOCO^-$ using 1.60 eV photons, evidence was seen in the photoelectron spectra for hot bands of ~0.3 eV relative to the theoretical predictions of the EA for $HOCO^-$.[80] This further supports the production of a vibrationally excited, and very possibly nonthermal, distribution of $HOCO^-$ and $DOCO^-$ anions in the source. This could explain the observation of the OH+CO

$+e^-$ channel above the theoretically predicted energetic limits for KE_{max} by DPD of these vibrationally "hot" $HOCO^-$. The experimental KE_{max} in $OH+CO+e^-$ is approximately 0.5 eV higher than the theoretical value, indicating the excitation of some of the parent anions by several quanta of C–O′ stretching, which may preferentially lead to the C–O′ bond breaking upon photodetachment and enhance the production of OH+CO. The tentative observation of a progression in the C–O′ stretch of $HOCO^-$ in the P(eKE) spectra for the $OH+CO+e^-$ channel mentioned in Sec. III further supports this mechanism.

The existence of vibrationally excited parent anions in the production of $OH+CO+e^-$ is also crucial in explaining the isotope effect observed in Fig. 3(b). In $DOCO^-$, the density of vibrational states is larger than in $HOCO^-$, so more vibrational excitation might be expected. Therefore, the shift in the P(eKE) of Fig. 3(b) to higher eKE is likely to arise from the increased population of vibrationally excited states in $DOCO^-$ and small isotopic shifts in the EA. The significant decrease of the O′–H stretching frequency[10] in the neutral radical upon deuteration will also contribute to the observed isotope shift in P(eKE) of Fig. 3(b), since the isotope shift of the vibrational frequencies in the anion is expected to be smaller due to the more anharmonic anionic PES. A detailed examination of this explanation requires extensive *ab initio* calculations for vibrational frequencies and ZPEs on a global PES of $HOCO^-$ and $DOCO^-$, beyond the scope of the present study. On the other hand, little isotope effect was observed in the $P(E_T)$ distributions for the recoil of OD +CO neutral products, consistent with a predicted simultaneous reduction of ZPEs and O–D stretching frequencies when OH and HOCO are deuterated.[10]

It should be noted that although the experimental KE_{max} (line II) in Fig. 3(a) is ~0.5 eV higher than the predicted value, the discrepancy between the theoretical KE_{max} and the most intense feature in the $P(\mathrm{eKE}, E_T)$ spectra of Fig. 3(a) is less than 0.3 eV. Assuming that a subset of the $HOCO^-$ anions are vibrationally excited by ~0.3 eV, the horizontal line set II representing the c-HOCO TS2 in Fig. 2(a) will be raised by the same amount, separating the two resolved structures annotated by "A" and "B" in the $H+CO_2+e^-P(\mathrm{eKE}, E_T)$ spectrum of Fig. 2(a). This raises the possibility that vibrationally excited $HOCO^-$ anions also play a role in the apparent production of $H+CO_2+e^-$ below the c-HOCO TS2 barrier. The $H+CO_2+e^-$ products may be formed by two different mechanisms simultaneously: (1) DPD of vibrationally excited $HOCO^-$ produces nascent HOCO radicals above the dissociation barrier, followed by rapid unimolecular dissociation into $H+CO_2$ [feature A in Fig. 2(a)]; and (2) nascent HOCO radicals formed by the photodetachment of $HOCO^-$ with less vibrational excitation that tunnel through the c-HOCO TS2 barrier to form $H+CO_2$ [feature B in Fig. 2(a)]. Assuming this mechanism, the spectrum in Fig. 2(b) indicates that in the case of $DOCO^-$, the vibrationally excited anions play a more important role in $D+CO_2$ formation (feature A dominates) while the probability of tunneling is reduced greatly in the case of the D atom (feature B essentially disappears). An immediate result of this explanation for the isotope effect is that most $D+CO_2$ fragments are formed by passing over the c-HOCO TS2 barrier, yielding a narrower eKE spectrum and a shift in the $P(E_T)$ distribution to higher E_T compared with the $H+CO_2+e^-$ channel that includes a significant tunneling contribution.

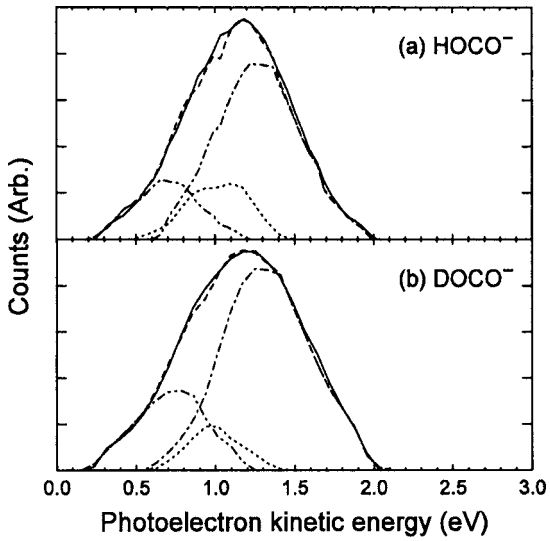

FIG. 5. The fitting of overall P(eKE) distributions (solid line) by the three channel-resolved P(eKE) spectra shown in Fig. 4. The dashed line represents the fitting result. The dash-dotted lines represent P(eKE) spectra in coincidence with stable HOCO/DOCO, with the dotted lines for the H/D $+CO_2$ and dot-dot-dashed lines for the OH/OD+CO channels. The areas of the three channel-resolved P(eKE) distributions are used to calculate relative branching ratios in the DPD of (a) $HOCO^-$ and (b) $DOCO^-$ at $E_{h\nu}$ =3.21 eV.

An alternative mechanism is that the $H+CO_2+e^-$ channel is solely produced by passing over the c-HOCO TS2 barrier during DPD of vibrationally excited $HOCO^-$ and there is no tunneling effect. This is less likely as it conflicts with the evidence for the tunneling mechanism from the measurement of the product branching ratios which will be discussed in detail below. In addition, this mechanism could not explain why feature A at eKE= ~0.9 eV and feature B at eKE= ~1.1 eV in the $H+CO_2+e^-$ channel merge into one narrower peak at eKE= ~1.0 eV in the $D+CO_2+e^-$ channel. Another possibility, mentioned earlier, that $C_{2v}H\cdot CO_2$ is involved in the formation of either feature A or B can also be neglected even in the presence of anions with vibrational excitation up to ~0.3 eV, as this is not sufficient to overcome the TS4 barrier leading to the formation of $C_{2v}H\cdot CO_2$. Therefore the only reasonable explanation is that upon deuterium substitution, feature B disappears as the tunneling mechanism is closed, while feature A formed by the photodetachment of vibrationally excited anions shifts to higher eKE as observed in the other two channels forming OD $+CO+e^-$ and $DOCO+e^-$.

The branching ratios for the three competing neutral product channels, stable HOCO, $H+CO_2$, and OH+CO, can help understand the reaction mechanisms discussed above. The most reliable approach to obtaining the branching ratios is to reproduce the overall P(eKE) spectra in Fig. 4(a) by fitting the three channel-resolved eKE distributions determined in the PPC experiment, as shown in Fig. 5. The branching ratios estimated by the eKE fitting in $HOCO^-$ and

TABLE II. Branching ratios in DPD of $HOCO^-$.

	Stable HOCO	$H+CO_2$	OH+CO
258 nm[a]	0.81	0.06	0.13
386 nm[b]	0.67	0.16	0.17
386 nm ($DOCO^-$)[b]	0.70	0.09	0.21
Theory *(trans)*[c]	0.86	0.03	0.11
Theory *(cis)*[c]	0.89	0.02	0.09

[a]Reference 60.
[b]The uncertainties of branching ratio are estimated to be ~10% of the listed value for the $H/D+CO_2$ and OH/OD+CO channels.
[c]Six-dimensional wave packet calculations, Ref. 64.

$DOCO^-$ measurements are listed in Table II, along with the results from a previous DPD study of $HOCO^-$ at 258 nm and the recent calculations.

In general, both experiment and theory show that the majority of the neutral products in the DPD process of $HOCO^-/DOCO^-$ are stable HOCO or DOCO radicals, qualitatively consistent with the deep potential energy well of HOCO. Comparison of the $H+CO_2+e^-$ and $D+CO_2+e^-$ channels at $E_{h\nu}=3.21$ eV shows a significant isotope effect as the branching ratio of this channel decreases by half in the deuterated measurement, consistent with a role for tunneling in this DPD channel as discussed above. An interesting observation is that the reduction of $D+CO_2$ fragments is accompanied by an increase in the production of both stable DOCO and OD+CO. This can be explained by the predicted isotope effect on the HOCO PES. As calculated by Yu *et al.*, the ZPE of the OD+CO dissociation limit decreases by 0.06 eV compared with OH+CO, while the tunneling barrier *c*-HOCO TS2 is only reduced by 0.02 eV upon deuterium substitution (see Table I).[10] As a result, on the DOCO PES, the OD+CO ground state is 0.09 eV lower than the TS2 barrier. Thus the excess nascent DOCO radicals arising from the elimination of tunneling would not only be trapped in the DOCO well but also dissociate into ground state OD+CO, causing a simultaneous increase in the branching ratios of both OD+CO and stable DOCO.

Recently, Zhang *et al.* calculated branching ratios resulting from the DPD of $HOCO^-$ using six-dimensional quantum wave packet dynamics on the LTSH surface.[64] The results are summarized in Table II for comparison with the experimental results. The theoretical work of Zhang *et al.* predicted that only 2%–3% of neutral products are $H+CO_2$, which differs significantly from the experimental values, 16% for $H+CO_2$ in DPD of $HOCO^-$ and 9% for $D+CO_2$ in DPD of $DOCO^-$. The theoretical branching ratio for OH+CO is also smaller than the experimental result. Consequently, the theoretical results predict that the stable HOCO product is more dominant. There are a number of potential explanations for these disagreements between theory and experiment. Based on the discussion above, the possible role played by vibrationally hot anions in the production of OH+CO and $H+CO_2$ products is neglected in these calculations. It was also found that the calculations effectively predict no tunneling leading to $H+CO_2$ products. This may be a consequence of the LTSH PES used in the wave packet calculation not being sufficiently accurate in the critical region around the TS2 barrier separating *cis*-HOCO from $H+CO_2$ products.[11] In fact, as discussed by Zhang *et al.*,[64] although the energy of the *c*-HOCO TS2 on the LTSH surface is similar to that obtained from other high-level *ab initio* calculations,[10] the LTSH surface predicts a thicker barrier, reducing the tunneling probability.[10,11] It should be noted as well that the LTSH surface was not optimized near the stationary points in the HOCO well and in fact had to be significantly rescaled to obtain a realistic Franck-Condon region.[60,64] Zhang *et al.* also carried out Rice-Ramsperger-Kassel-Marcus calculations on the branching ratios, yielding a ratio of 1:1.2 for $OH+CO:H+CO_2$. This is close to the ratio of 1.1:1 we found in the present $E_{h\nu}=3.21$ eV DPD experiments on $HOCO^-$, but very different from the 2:1 ratio obtained in CCF's measurement using 4.80 eV photons.[60] The discrepancy between the two measurements at different photon energies is likely to be a result of the improved eKE resolution using a lower photon energy and the reduction of false oincidences by additional mass gating on the photofragment channels. It is clear that in spite of the impressive full-dimensional calculations of Zhang *et al.*, a complete understanding of the DPD dynamics observed in these experiments will require more theoretical work. Accurate simulation of a DPD experiment requires fully characterized anion and neutral surfaces. In the case of the present experiments, the potential existence of vibrationally excited anions makes the characterization of the anion surface even more important. A faithful representation of the present experimental results, including vibrationally excited $HOCO^-$, would require a reliable anion PES for *trans*- and *cis*-$HOCO^-$ in a range up to the OH^-+CO dissociation limit.

The wave packet calculations of Zhang *et al.* also predicted energy distributions for the DPD of $HOCO^-$. In their results, the P(eKE) spectra for $H+CO_2+e^-$ channel shift ~0.5 eV to higher eKE from the experimental data. This is not surprising as vibrationally excited $HOCO^-$ anions were not taken into account and negligible tunneling was found in their work. Owing to the approach used by Zhang *et al.*, no prediction of the $P(E_T)$ for the $H+CO_2$ product channel was obtained. On the other hand, the theoretical $P(E_T)$ distributions for OH+CO products are consistent with the experiment, implying that the DPD of the ground state and vibrationally excited $HOCO^-$ produces nascent neutral HOCO radicals with very similar dissociation dynamics, possibly a result of significant vibrational adiabaticity on the neutral dissociation surface. Due to the limited Franck-Condon region predicted by the LTSH PES for neutral HOCO and the harmonic anion surface in the calculation of Zhang *et al.*, the DPD events they predicted mostly occur from the long tail extending towards the high energy side of the spectral density (Fig. 3 in Ref. 64). Therefore, a significant effect on the two DPD channels is expected if a more realistic Franck-Condon region, including vibrationally excited anions on an anharmonic surface, becomes available.

V. CONCLUSIONS

Photoelectron-photofragment coincidence spectroscopy was employed to study the DPD dynamics of $HOCO^-$ and

$DOCO^-$ at $E_{h\nu}$=3.21 eV, providing a useful method to probe the dynamics of the $OH+CO \rightarrow HOCO^* \rightarrow H+CO_2$ reaction on the ground state potential energy surface. The dominant neutral product formed by photodetachment was found to be stable HOCO/DOCO free radicals trapped in a deep potential well, accompanied by two dissociation channels leading to $H/D+CO_2$ and OH/OD+CO products. It is suggested that both OH+CO and OD+CO products are formed by the DPD of vibrationally excited $HOCO^-/DOCO^-$. $H+CO_2$ products are produced by either the tunneling mechanism at total energies below the predicted dissociation barrier *c*-HOCO TS2 or unimolecular dissociation of nascent HOCO radicals above the *c*-HOCO TS2, formed by DPD of vibrationally excited $HOCO^-$. As a result, two resolved structures are observed in the PPC spectrum for $H+CO_2+e^-$. Tunneling is reduced significantly in the $DOCO^-+h\nu \rightarrow D+CO_2+e^-$ DPD process and the vibrationally excited $DOCO^-$ anions become the major source of $D+CO_2$ products. The results presented in this study provide evidence in favor of the tunneling mechanism suggested by some of the previous kinetics studies on the $OH+CO \rightarrow H+CO_2$ reaction at low temperature.[6,12,16,37] The proposed DPD mechanism is also supported by the product branching ratios. The recent quantum wave packet dynamics predictions of Zhang *et al.* illustrate that full-dimensionality calculations on this four-atom system are now possible and can capture essential elements of the experimental results. More extensive calculations, however, are necessary for a detailed evaluation of the DPD mechanisms suggested by this study. In particular, accurate *ab initio* calculations to construct a complete anharmonic potential energy surface of $HOCO^-$ up to the OH^-+CO dissociation limit, as well as the stationary points for $DOCO^-$, are needed. In addition, the LTSH surface used in the simulations has known problems with the stationary points at the bottom of the HOCO well, so an improved neutral surface is also required. From an experimental perspective, a primary goal should be the elimination of any hot band contributions in the parent anions. A temperature-controlled ion trap for anion accumulation and cooling may be the best approach to solving this problem, as illustrated in a number of studies by Wang *et al.*[79] Near-threshold photodetachment studies of $HOCO^-$ and $DOCO^-$ at a photon energy of 1.6 eV, characterizing the bottom of the HOCO well, will also be reported in the near future.[80]

ACKNOWLEDGMENTS

This work was supported by the Department of Energy (DOE) under the Grant No. DE-FG03-98ER14879. One of the authors (R.E.C.) acknowledges many useful discussions with Evelyn Goldfield and Stephen Gray.

[1] T. Rockmann, C. A. M. Brenninkmeijer, G. Saueressig, P. Bergamaschi, J. N. Crowley, H. Fischer, and P. J. Crutzen, Science **281**, 544 (1998).
[2] J. A. Miller, R. J. Kee, and C. K. Westbrook, Annu. Rev. Phys. Chem. **41**, 345 (1990).
[3] A. D. McLean and Y. Ellinger, Chem. Phys. Lett. **98**, 453 (1983).
[4] A. D. McLean and Y. Ellinger, Chem. Phys. **94**, 25 (1985).
[5] T. V. Duncan and C. E. Miller, J. Chem. Phys. **113**, 5138 (2000).
[6] R. S. Zhu, E. G. W. Diau, M. C. Lin, and A. M. Mebel, J. Phys. Chem. A **105**, 11249 (2001).
[7] G. C. Schatz, M. S. Fitzcharles, and L. B. Harding, Faraday Discuss. Chem. Soc. **84**, 359 (1987).
[8] K. Kudla, G. C. Schatz, and A. F. Wagner, J. Chem. Phys. **95**, 1635 (1991).
[9] K. S. Bradley and G. C. Schatz, J. Chem. Phys. **106**, 8464 (1997).
[10] H.-G. Yu, J. T. Muckerman, and T. J. Sears, Chem. Phys. Lett. **349**, 547 (2001).
[11] M. J. Lakin, D. Troya, G. C. Schatz, and L. B. Harding, J. Chem. Phys. **119**, 5848 (2003).
[12] M. Aoyagi and S. Kato, J. Chem. Phys. **88**, 6409 (1988).
[13] Y. M. Li and J. S. Francisco, J. Chem. Phys. **113**, 7963 (2000).
[14] R. Valero, M. C. Van Hemert, and G.-J. Kroes, Chem. Phys. Lett. **393**, 236 (2004).
[15] X. Song, J. Li, H. Hou, and B. Wang, J. Chem. Phys. **125**, 094301 (2006).
[16] M. J. Frost, P. Sharkey, and I. W. M. Smith, J. Phys. Chem. **97**, 12254 (1993).
[17] K. Kudla, A. G. Koures, L. B. Harding, and G. C. Schatz, J. Chem. Phys. **96**, 7465 (1992).
[18] M. I. Lester, B. V. Pond, M. D. Marshall, D. T. Anderson, L. B. Harding, and A. F. Wagner, Faraday Discuss. **118**, 373 (2001).
[19] D. E. Milligan and M. E. Jacox, J. Chem. Phys. **54**, 927 (1971).
[20] M. E. Jacox, J. Chem. Phys. **88**, 4598 (1988).
[21] D. Forney, M. E. Jacox, and W. E. Thompson, J. Chem. Phys. **119**, 10814 (2003).
[22] B. Ruscic, M. Schwarz, and J. Berkowitz, J. Chem. Phys. **91**, 6780 (1989).
[23] H. E. Radford, W. Wei, and T. J. Sears, J. Chem. Phys. **97**, 3989 (1992).
[24] T. J. Sears, W. M. Fawzy, and P. M. Johnson, J. Chem. Phys. **97**, 3996 (1992).
[25] T. J. Sears, H. E. Radford, and M. A. Moore, J. Chem. Phys. **98**, 6624 (1993).
[26] H. E. Radford, M. A. Moore, T. J. Sears, J. Grussdorf, J. Nolte, and F. Temps, J. Mol. Spectrosc. **165**, 137 (1994).
[27] J. T. Petty and C. B. Moore, J. Mol. Spectrosc. **161**, 149 (1993).
[28] J. T. Petty and C. B. Moore, J. Chem. Phys. **99**, 47 (1993).
[29] A. Miyoshi, H. Matsui, and N. Washida, J. Chem. Phys. **100**, 3532 (1994).
[30] M. E. Greenslade, M. Tsiouris, R. T. Bonn, and M. I. Lester, Chem. Phys. Lett. **354**, 203 (2002).
[31] M. D. Marshall, B. V. Pond, and M. I. Lester, J. Chem. Phys. **118**, 1196 (2003).
[32] M. J. Frost, P. Sharkey, and I. W. M. Smith, Faraday Discuss. **91**, 305 (1991).
[33] D. Fulle, H. F. Hamann, H. Hippler, and J. Troe, J. Chem. Phys. **105**, 983 (1996).
[34] D. M. Golden, G. P. Smith, A. B. McEwen, C. L. Yu, B. Eiteneer, M. Frenklach, G. L. Vaghjiani, A. R. Ravishankara, and F. P. Tully, J. Phys. Chem. A **102**, 8598 (1998).
[35] J. P. Senosiain, C. B. Musgrave, and D. M. Golden, Int. J. Chem. Kinet. **35**, 464 (2003).
[36] J. P. Senosiain, S. J. Klippenstein, and J. A. Miller, Appl. Categ. Struct. **30**, 945 (2005).
[37] W. C. Chen and R. A. Marcus, J. Chem. Phys. **123**, 094307 (2005).
[38] G. Paraskevopoulos and R. S. Irwin, J. Chem. Phys. **80**, 259 (1984).
[39] G. Paraskevopoulos and R. S. Irwin, Chem. Phys. Lett. **93**, 138 (1982).
[40] D. M. Sonnenfroh, R. G. Macdonald, and K. Liu, J. Chem. Phys. **94**, 6508 (1991).
[41] M. Alagia, N. Balucani, P. Casavecchia, D. Stranges, and G. G. Volpi, J. Chem. Phys. **98**, 8341 (1993).
[42] M. C. van Beek, K. Schreel, and J. J. ter Meulen, J. Chem. Phys. **109**, 1302 (1998).
[43] C. Y. Shi, L. Ren, and F. A. Kong, ChemPhysChem **7**, 820 (2006).
[44] N. F. Scherer, C. Sipes, R. B. Bernstein, and A. H. Zewail, J. Chem. Phys. **92**, 5239 (1990).
[45] S. K. Shin, C. Wittig, and W. A. Goddard, J. Phys. Chem. **95**, 8048 (1991).
[46] S. I. Ionov, G. A. Brucker, C. Jaques, L. Valachovic, and C. Wittig, J. Chem. Phys. **99**, 6553 (1993).
[47] G. W. Flynn and R. E. Weston, J. Phys. Chem. **97**, 8116 (1993).
[48] M. Brouard, I. Burak, D. W. Hughes, K. S. Kalogerakis, J. P. Simons, and V. Stavros, J. Chem. Phys. **113**, 3173 (2000).
[49] D. C. Clary and G. C. Schatz, J. Chem. Phys. **99**, 4578 (1993).
[50] D. M. Medvedev, S. K. Gray, E. M. Goldfield, M. J. Lakin, D. Troya, and

G. C. Schatz, J. Chem. Phys. **120**, 1231 (2004).
[51] E. M. Goldfield, S. K. Gray, and G. C. Schatz, J. Chem. Phys. **102**, 8807 (1995).
[52] D. H. Zhang and J. Z. H. Zhang, J. Chem. Phys. **103**, 6512 (1995).
[53] F. N. Dzegilenko and J. M. Bowman, J. Chem. Phys. **105**, 2280 (1996).
[54] H. G. Yu and J. T. Muckerman, J. Chem. Phys. **117**, 11139 (2002).
[55] D. A. McCormack and G. J. Kores, Chem. Phys. Lett. **373**, 648 (2003).
[56] R. Valero, D. A. McCormack, and G. J. Kroes, J. Chem. Phys. **120**, 4263 (2004).
[57] R. R. Bernecker and F. A. Long, J. Phys. Chem. **65**, 1565 (1961).
[58] M. A. Haney and J. L. Franklin, Trans. Faraday Soc. **65**, 1794 (1969).
[59] B. Ruscic and M. Litorja, Chem. Phys. Lett. **316**, 45 (2000).
[60] T. G. Clements, R. E. Continetti, and J. S. Franciso, J. Chem. Phys. **117**, 6478 (2002).
[61] T. M. Miller, A. A. Viggiano, A. E. S. Miller, R. A. Morris, M. Henchman, J. F. Paulson, and J. M. Vandoren, J. Chem. Phys. **100**, 5706 (1994).
[62] D. A. Dixon, D. Feller, and J. S. Francisco, J. Phys. Chem. A **107**, 186 (2003).
[63] D. Feller, D. A. Dixon, and J. S. Francisco, J. Phys. Chem. A **107**, 1604 (2003).
[64] S. Zhang, D. M. Medvedev, E. M. Goldfield, and S. K. Gray, J. Chem. Phys. **125**, 164312 (2006).
[65] R. E. Continetti, Int. Rev. Phys. Chem. **17**, 227 (1998).
[66] J. A. Davies, J. E. LeClaire, R. E. Continetti, and C. C. Hayden, J. Chem. Phys. **111**, 1 (1999).
[67] J. A. Davies, R. E. Continetti, D. W. Chandler, and C. C. Hayden, Phys. Rev. Lett. **84**, 5983 (2000).
[68] M. S. Bowen and R. E. Continetti, J. Phys. Chem. A **108**, 7827 (2004).
[69] M. S. Bowen, M. Becucci, and R. E. Continetti, J. Phys. Chem. A **109**, 11781 (2005).
[70] D. P. DeBruijn and J. Los, Rev. Sci. Instrum. **53**, 1020 (1982).
[71] R. E. Continetti, D. R. Cyr, D. L. Osborn, D. J. Leahy, and D. M. Neumark, J. Chem. Phys. **99**, 2616 (1993).
[72] B. L. Peko and T. M. Stephen, Nucl. Instrum. Methods Phys. Res. B **171**, 597 (2000).
[73] T. G. Clements, Ph.D. thesis, University of California, San Diego, 2002.
[74] G. Herzberg, *Molecular Spectra and Molecular Structure II. Infrared and Raman Spectra of Polyatomic Molecules* (Krieger, Malabar, FL, 1991).
[75] T. G. Clements and R. E. Continetti, J. Chem. Phys. **115**, 5345 (2001).
[76] E. H. Kim, S. E. Bradforth, D. W. Arnold, R. B. Metz, and D. M. Neumark, J. Chem. Phys. **103**, 7801 (1995).
[77] J. B. Kim, P. G. Wenthold, and W. C. Lineberger, J. Chem. Phys. **108**, 830 (1998).
[78] Z. Lu and R. E. Continetti, J. Phys. Chem. A **108**, 9962 (2004).
[79] X. B. Wang, H. K. Woo, L. S. Wang, B. Minofar, and P. Jungwirth, J. Phys. Chem. A **110**, 5047 (2006).
[80] Z. Lu and R. E. Continetti (unpublished).
[81] J. R. Smith, J. B. Kim, and W. C. Lineberger, Phys. Rev. A **55**, 2036 (1997).
[82] B. Ruscic, A. F. Wagner, L. B. Harding *et al.*, J. Phys. Chem. A **106**, 2727 (2002).
[83] K. R. Lykke, K. K. Murray, and W. C. Lineberger, Phys. Rev. A **43**, 6104 (1991).